Applied Surface Science 500 (2020) 144041

Contents lists available at ScienceDirect

Applied Surface Science

journal homepage: www.elsevier.com/locate/apsusc

Full Length Article

Achieving ultralow surface roughness and high material removal rate in fused silica *via* a novel acid SiO_2 slurry and its chemical-mechanical polishing mechanism

Xiao-Lei Shi[a,b,c,1], Gaopan Chen[a,d,e,1,*], Li Xu[a], Chengxi Kang[a], Guihai Luo[a,d,e], Haimei Luo[a,d,e], Yan Zhou[a,d,e], Matthew S. Dargusch[c], Guoshun Pan[a,d,e,*]

[a] State Key Laboratory of Tribology, Tsinghua University, Beijing 100084, China
[b] Centre for Future Materials, University of Southern Queensland, Springfield, Queensland 4300, Australia
[c] School of Mechanical and Mining Engineering, The University of Queensland, Brisbane, Queensland 4072, Australia
[d] Guangdong Provincial Key Laboratory of Optomechatronics, Shenzhen 518057, China
[e] Shenzhen Key Laboratory of Micro/Nano Manufacturing, Research Institute of Tsinghua University in Shenzhen, Shenzhen 518057, China

ARTICLE INFO

Keywords:
Fused silica
Chemical-mechanical polishing
Acid silica slurry
Material removal rate
Surface roughness

ABSTRACT

Fused silica is widely used as a substrate material in various optical precision devices, and its surface quality plays a significant role in determining the optical performance. However, it is difficult to achieve an ultra-smooth surface without obvious damage using traditional planarization techniques. In this work, we report on the simultaneous achievement of ultralow surface roughness of ~0.193 nm and high material removal rate of ~10.9 μm h^{-1} on a fused silica substrate *via* a novel acid SiO_2 slurry. The results show an improvement of removal rate by ~900% compared to its alkaline counterpart. Comprehensive studies based on thermogravimetric analysis, infrared X-ray photoelectron spectroscopy, and nuclear magnetic resonance spectra reveal that phenolic hydroxyl in the acid SiO_2 slurry plays a critical role in achieving high material removal rate during the chemical-mechanical polishing process, by well-distributing the SiO_2 abrasives with an average size of only ~80 nm. This approach delivers the high surface quality. Evidence in support of this explanation has been obtained using advanced characterization techniques including scanning electron microscopy, atomic force microscopy, and optical interferometry profiling. This novel acid SiO_2 slurry is also environmentally friendly with significantly higher durability and stability, which is especially suitable for industrial scale production.

1. Introduction

Transparent fused silica (FS) glass possesses excellent permeability in the ultraviolet, visible and near infrared spectral regions with a wavelength range from 185 nm to 3500 nm [1–3]. With unique advantages including significant high temperature resistance [4], low thermal expansion coefficient [5], and stable chemical and radiation resistance [6,7], FS has been treated as a good candidate substrate material with great potential in various optical precision devices applied in aerospace [8], detection systems [9], spectroscopy instruments [10], and light guide communications [11]. Processes of cutting, grinding, and polishing are generally performed before FS is assembled into devices [12–15]. For the polishing process which directly determines the surface quality of FS [16], it is of significance because the surface roughness plays a dominant role in determining the optical performance of devices using an appropriate laser damage threshold [17,18]. However, it is difficult to achieve an ultra-smooth surface without damage using traditional planarization techniques and this has hampered the realization of high surface quality on FS.

Chemical-mechanical polishing (CMP) is well known to be one of the most advanced planarization techniques to realize atomic-level ultra-smooth surface on various materials [19], including silicon wafers [20], copper [21], glass [22], sapphire [23–28], silicon carbide (SiC) [25,29–33], and gallium nitride (GaN) [34–36]. In a typical CMP process, a corrosive chemical slurry including abrasives is used, and the chemical products formed on the material surface can be simultaneously removed by the abrasives, resulting in a flat surface. For its applications on FS polishing, previous results show that an alkaline

* Corresponding authors at: Shenzhen Key Laboratory of Micro/Nano Manufacturing, Research Institute of Tsinghua University in Shenzhen, Shenzhen 518057, China.
E-mail addresses: chengaopan2006@126.com, chengaopan@126.com (G. Chen), pangs@tsinghua.edu.cn (G. Pan).
[1] These authors contribute equally to this work.

https://doi.org/10.1016/j.apsusc.2019.144041
Received 25 May 2019; Received in revised form 31 August 2019; Accepted 14 September 2019
Available online 01 October 2019
0169-4332/

cerium oxide (CeO_2) based slurry can realize a high material removal rate (MRR) of $> 10\,\mu m\,h^{-1}$ [37]. The MRR of fused silica can be calculated as [38]:

$$MRR = \frac{10^7 \Delta m}{\pi \times r^2 \times \rho \times t} \quad (1)$$

where Δm is the removal weight of fused flat silica, ρ is the density of fused silica ($2.2\,g\,cm^{-3}$), r is the radius of flat fused silica, and t is polishing time. Even though the MRR achieved using the CeO_2-based slurry is promising, the final surface roughness Rq of > 0.4 nm is still high [37], and the devices cannot meet the surface roughness requirements required for assembly and incorporation into devices. Meanwhile, CeO_2 is a typical toxic chemical [39,40], which can easily contaminate the working environment during usage and harm the human body [41,42], thus it is not suitable for long-term fabrications To solve this problem, silica (SiO_2) is an alternative candidate. Novel environment-friendly silica slurries have been developed in CMP to polish metal [43], alloys [44–46], and semiconductors [47,48] used for high performance devices, eliminating the environmental contamination and reducing potential harmful impact on operators. These studies represent both a breakthrough and the achievement of a milestone in the development of traditional machining and manufacturing. Different from CeO_2 abrasives which have irregular shapes and sharp edges [49], the environmentally friendly SiO_2 abrasives possess more regular ball-like shapes and sizes [27,29], which have less potential to cause damage and/or defects such as scratches on the polished surface during CMP. However, even though the surface quality is significantly improved with a low Rq of < 0.2 nm by using alkaline SiO_2 based slurry, a significantly lower MRR of only $\sim 1.0\,\mu m\,h^{-1}$ restricts its application for industrial scale-up. Therefore, an improved formulation based on a SiO_2 slurry is needed in order to boost the low MRR and keep the high surface quality of FS over the same period.

In this work, we report on a novel acid based SiO_2 slurry which can simultaneously realize an ultralow Rq of only ~0.193 nm and a high MRR of $\sim 10.9\,\mu m\,h^{-1}$ on the FS substrate. This process represents an improvement by ~900% compared to its alkaline counterpart. To explore the fundamental mechanisms behind the achievement of such high CMP performance, we performed comprehensive characterization including scanning electron microscopy (SEM), atomic force microscopy (AFM), and optical interference profilometry (OIP) in order to study both the abrasives and the FS surface quality that can be achieved by these abrasives. In addition, thermogravimetric analysis (TGA), infrared (IR) spectra, X-ray photoelectron spectroscopy (XPS), nuclear magnetic resonance (NMR) spectra, and ion chromatography (IC) where utilized in order to study the key features that determine the high MRR produced *via* using such a novel acid SiO_2 slurry. Furthermore, the CMP performance *via* slurries for both new solution and slurries that had been standing for 1 month were also evaluated in order to study the stability of the abrasive slurry materials. The results indicate that phenolic hydroxyl in the acid SiO_2 slurry plays a critical role in achieving high MRR, and the well-distributed nano-sized SiO_2 abrasives contribute to such a low Rq. Meanwhile, significantly higher durability and stability were confirmed, indicating that our acid SiO_2 slurry is especially suitable for scale up to industrial production.

2. Experiments

2.1. Samples preparation

Several two-inch commercial FS wafers (Corning, USA) were used. The wafers were ~50.8 mm in diameter and ~5 mm in thickness, and had been preliminarily polished by double side lapping techniques in order to achieve highly planar and parallel surfaces on the two sides. The wafers were polished using a 1000S precision polishing machine (Kengjing Corporation), and several polyurethane (PU) polishing pads were used for CMP, that were purchased from Fujimi Corporation with type SURFIN 000. Amorphous SiO_2 abrasives were purchased from Nalco Co., Ltd. (type Nalco 2360), and CeO_2 abrasives were purchased from Baotou City Jiaxin Nanometre Materials Co., Ltd. The SiO_2 and CeO_2 were dispersed into pure water into a concentration of 5%. For the acid SiO_2 slurry, the active ingredient was ~1% phenol, and the pH of the slurry was adjusted to ~2 by ~0.3% tartaric acid before use. For the alkaline SiO_2 and CeO_2 slurries, ~1% phenol was also added into the slurries for comparison, and the pH of the slurries were adjusted to ~10 by using NaOH. The slurries were all supplied at a rate of $30\,ml\,min^{-1}$. The rotating speeds were 50 and 150 rpm for the upper dynamic polishing head and the down polishing stage [50], respectively. The pressure used during polishing was $100\,g\,cm^{-2}$. Each polishing period was for 1 h. After polishing, the FS was ultrasonically rinsed with a homemade cleaning agent (Patent CN 108048227 A) for 5 min and dried with a stream of air before characterization and/or measurements. To avoid glazing during CMP, between each polishing step, grinding with a diamond grinding disc (3M, US) for 5 min grinding was performed, followed by 5 min washing in pure water [50].

2.2. Samples characterizations

The polished FS wafers were characterized using a Leica DM2500 OM (Leica Microsystems Pty Ltd). The surface morphologies and surface roughness Rq were evaluated by AFM (Bruker Dimension Icon) and OIP (Zygo New View 7200). For OIP, the achieved images were obtained using a scan area of 15 μm × 15 μm. For AFM, silicon (Si) based tapping mode probes (NSG11 series, NT-MDT) were used for imaging. The tips from these AFM probes possess a typical tip radius of 10 nm, an aspect ratio of 3:1, a tip height of 10–15 μm, and a tip cone angle of $< 22^\circ$. The reflective side of the cantilever for laser reflection is covered by gold (Au). The typical resonant frequency is 255 kHz, and the force constant is from 5.5 to $22.5\,N\,m^{-1}$. The scan rate of AFM was 0.8 Hz, the set-point value for imaging was 150 mv, the scanning area was 10 × 10 μm, and the scan size was 768 × 768 points. The working temperature was kept at 25 °C. The polished and soaked FS samples were characterized by IR spectra (VERTEX 70, Bruker) and TGA (STA-449 F3). The soaking time for each slurry was 6 h.

The abrasives were dried from their corresponding slurries in a vacuum environment at room temperature (RT) before characterization. These abrasives were characterized using SEM (TESCAN MIRA3), TGA (STA-449 F3), IR spectra (VERTEX 70, Bruker), XPS (PHI Quantera II, Ulvac-Phi Inc.), and NMR (Avance III 400, Bruker, Germany). The slurries were characterized by IC (761 Compact, Metrohm). The particle size in the slurries were determined using a laser particle size analyzer (NanoS, Malvern).

3. Results and discussion

To evaluate the CMP performance on the FS substrate *via* different slurries, comprehensive studies based on an SEM, using a laser particle size analyzer (LPSA), and AFM, were investigated. Fig. 1(a–b) shows the typical SEM images of CeO_2 and SiO_2 abrasives with corresponding magnified SEM images inset, respectively. It is clearly seen that CeO_2 abrasives possess irregular shapes and that they easily agglomerate to form much larger particles. On the contrary, SiO_2 abrasives have much more regular round shapes and remain independent for each particle. Fig. 1(c) also compares their size distributions *via* LPSA. It is obvious that the measured average particle size Z of CeO_2 is ~1.5 μm due to agglomeration, much larger than that of SiO_2 which is only ~80 nm. Meanwhile, there are also slight peaks at ~15 μm and ~85 μm for CeO_2, indicating significant agglomeration in the slurry. For SiO_2 abrasives in both alkaline and acid slurries, there is only 1 peak for each slurry, indicating that there is no agglomeration for SiO_2 abrasives in both alkaline and acid slurries, which should produce benefits by avoiding surface damage on the FS substrate during CMP. Fig. 1(d–f) show

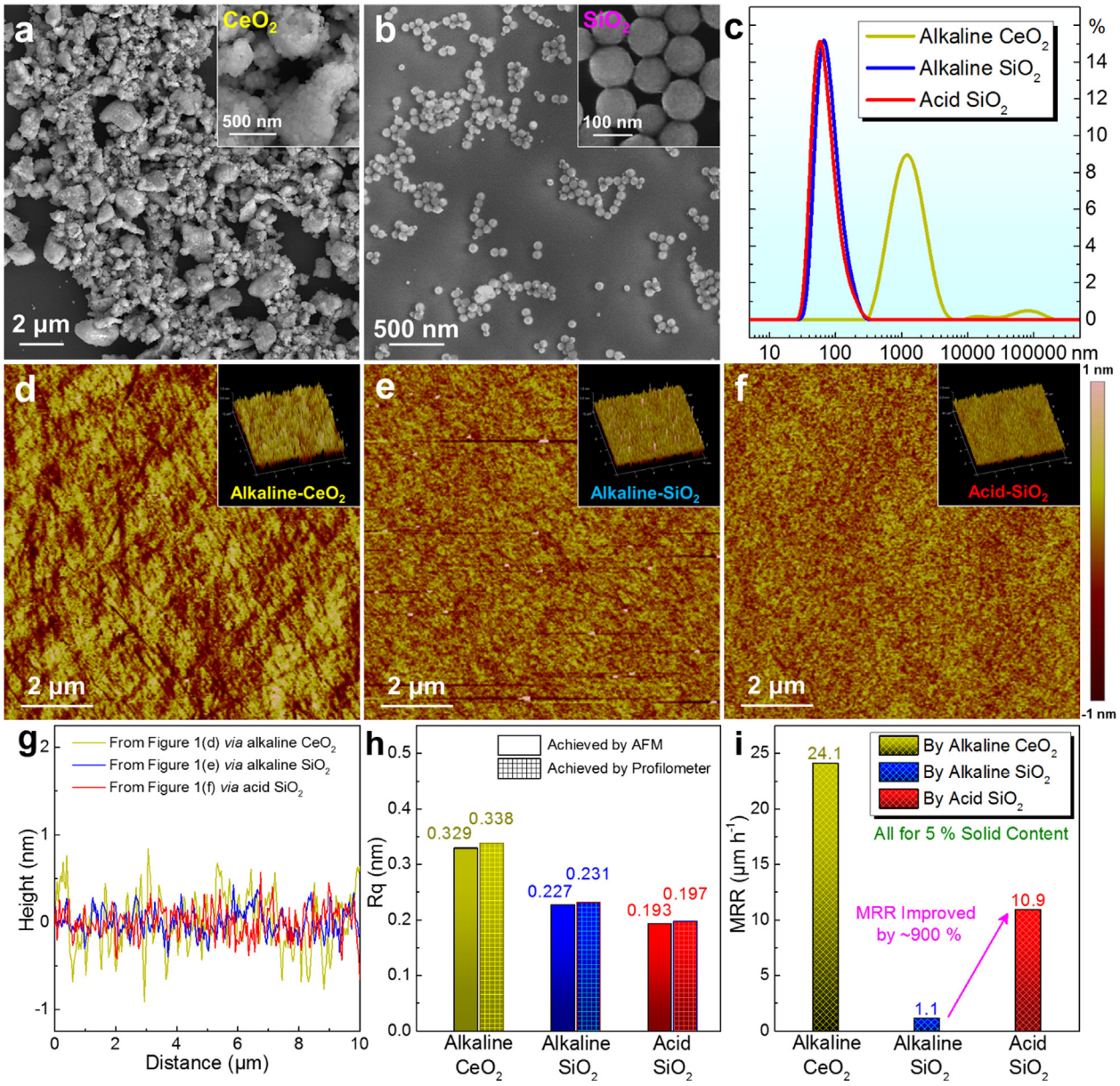

Fig. 1. Characterization of polishing abrasives and their CMP results. SEM images of (a) CeO_2 and (b) SiO_2 abrasives with corresponding magnified SEM images inset; (c) comparison of the size distribution curves of CeO_2 in alkaline slurry and SiO_2 in both alkaline and acid slurries; AFM images with the corresponding 3D images (inset) of the FS wafer surface after polishing by (d) alkaline CeO_2 slurry, (e) alkaline SiO_2 slurry, and (f) acid SiO_2 slurry; comparisons of (g) section lines taken from parts (d-f), (h) Rq, and (i) MRR by these slurries.

typical AFM images alongside the corresponding 3D images (inset) of the FS wafer surface after polishing using alkaline CeO_2 slurry, alkaline SiO_2 slurry, and acid SiO_2 slurry, respectively. It is clear that the surface polished *via* alkaline CeO_2 slurry is still rough with significant scratches caused by the CeO_2 abrasives during CMP. On the contrary, the surfaces polished *via* the SiO_2 slurry are much smoother without any obvious damage, indicating that SiO_2 abrasives are more suitable for achieving ultra-smooth surfaces on the FS substrate *via* CMP. However, compared with the acid SiO_2 slurry, there are several white abrasives that have adhered to the surface after polishing with the alkaline SiO_2 slurry, indicating that the acid SiO_2 slurry shows improved performance compared to the alkaline SiO_2 slurry in order to achieve uncontaminated FS surface. Fig. 1(g) also compares the section lines taken from Fig. 1(d–f), from which the surface polished *via* alkaline CeO_2 slurry is much rougher than that polished *via* SiO_2 slurries, indicating a much higher surface roughness. To evaluate this, Fig. 1(h) provides the measured Rq values *via* both AFM and OIP. Since both the AFM and OIP techniques can obtain surface roughness values with significantly higher accuracies, we can compare the measured Rq achieved using both equipment despite the fact that the measurement principles behind the two techniques are different. The results indicate that the acid SiO_2 slurry can contribute to an ultra-low Rq of only 0.193 nm on the polished FS surface, confirming that the acid SiO_2 slurry is much more suitable for achieving an ultra-smooth surface on the FS substrate. It should also be noted that the Rq values acquired from AFM are slightly lower than that from OIP, this phenomenon is mainly due to the potential wear of the AFM probe which may underestimate the measured Rq during scanning [27,28,51,52]. At the same time, the scanning areas for AFM and OIP are 10 μm × 10 μm and 15 μm × 15 μm, respectively. The observation for the scanning area of OIP is larger than that of AFM, is one of the reasons behind the differences in the measured Rq. Corresponding optical microscopy (OM) and OIP results of the FS substrate before and after polishing using different slurries are also provided in Figs. S1 and S2 in the Supporting Information for further reference.

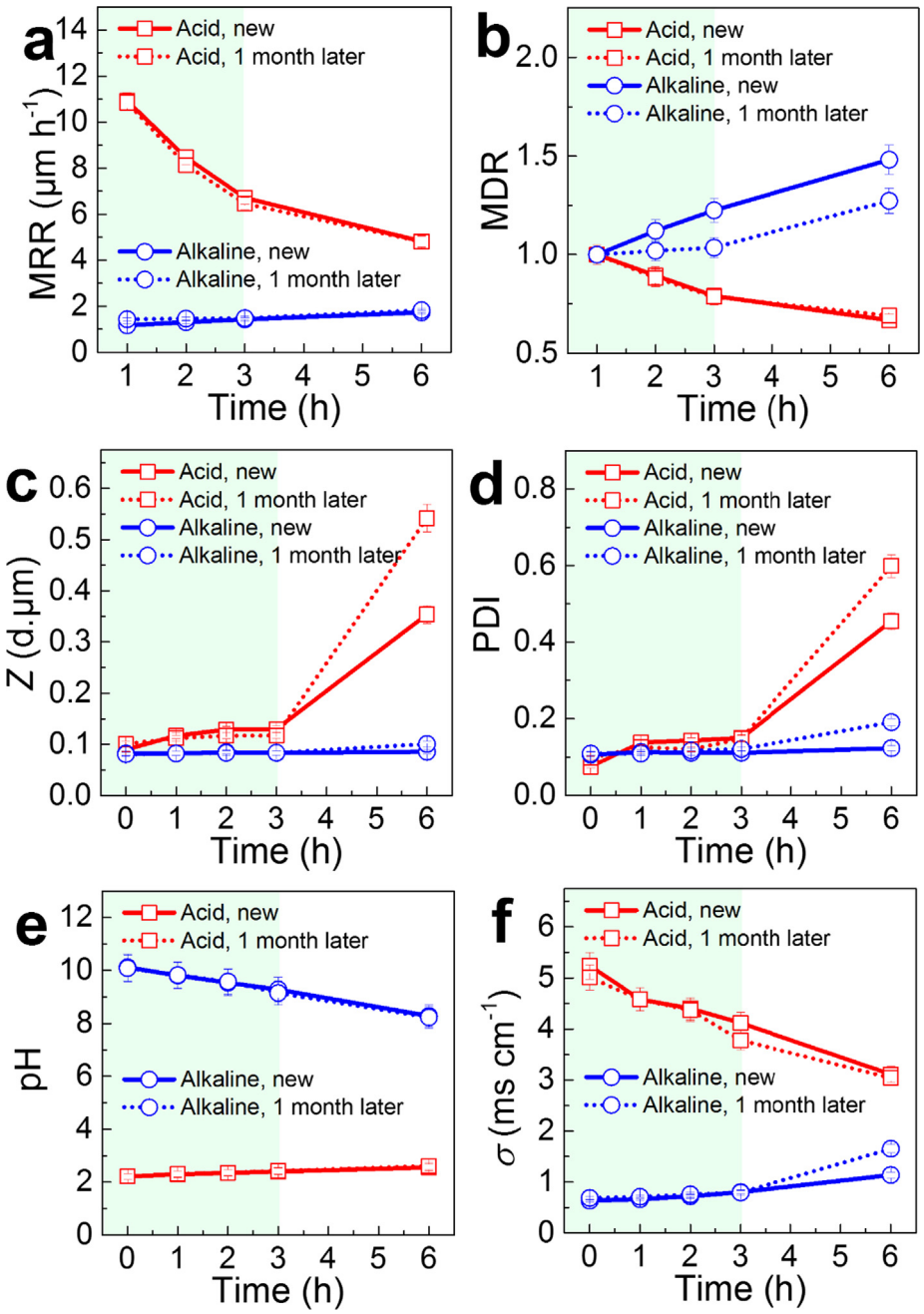

Fig. 2. Performance evaluations for both acid and alkaline SiO_2 slurries within 6 h (h) polishing: (a) MRR, (b) MDR, (c) *Z*, (d) PDI, (e) pH, and (f) *σ*. The performance of slurries standing for 1 month are also provided for comparison.

Even though the SiO_2 slurry can realize an ultra-smooth surface on the FS substrate, an appropriate MRR is still needed because the slurry should meet the requirements of industrial scale production. Fig. 1(i) compares the MRR of FS substrate during CMP *via* different slurries. It is clear that the acid SiO_2 slurry possesses a much higher MRR of ~10.9 μm h^{-1} than its alkaline counterpart (~1.1 μm h^{-1}), indicating that our novel acid SiO_2 slurry can simultaneously achieve excellent surface quality and high MRR, showing good potential for application into industrial scale production. At the same time, we also studied the effect of pH over a relatively wide range from ~2 to ~10, and the results show that with increasing pH, the MRR was obviously decreased but the Rq remained almost stable (Fig. S3), this is because the abrasives are the same in both acid and alkaline slurries, which are regular SiO_2 particles with an average size of only ~80 nm, thus the Rq is quite similar under different pH values when the MRR is not very high (compared to the CeO_2 slurry). To further evaluate the durability and stability of our SiO_2 slurries (both acid and alkaline slurries), a series of other property measurements and characterization procedures were performed including MRR, mass decline rate (MDR, defined as the ratio of MRR after and before 1 h (h) polishing), average particle size *Z*, polydispersity index (PDI, a measure of the distribution of molecular mass), pH, and electrical conductivity *σ*, as shown in Fig. 2(a–f), respectively. The circular polishing process was maintained for 6 h for each slurry, and the slurries that had been left standing for 1 month were also evaluated in order to study their stabilities, which are provided in Fig. 2 for comparison. Here the circular polishing process means that the slurry used in CMP was collected and re-used during polishing as part of a cyclical utilization strategy within a certain polishing time. From Fig. 2(a) and (b), it is clear that with increasing polishing time, the MRR from the acid SiO_2 slurry decreases, indicating

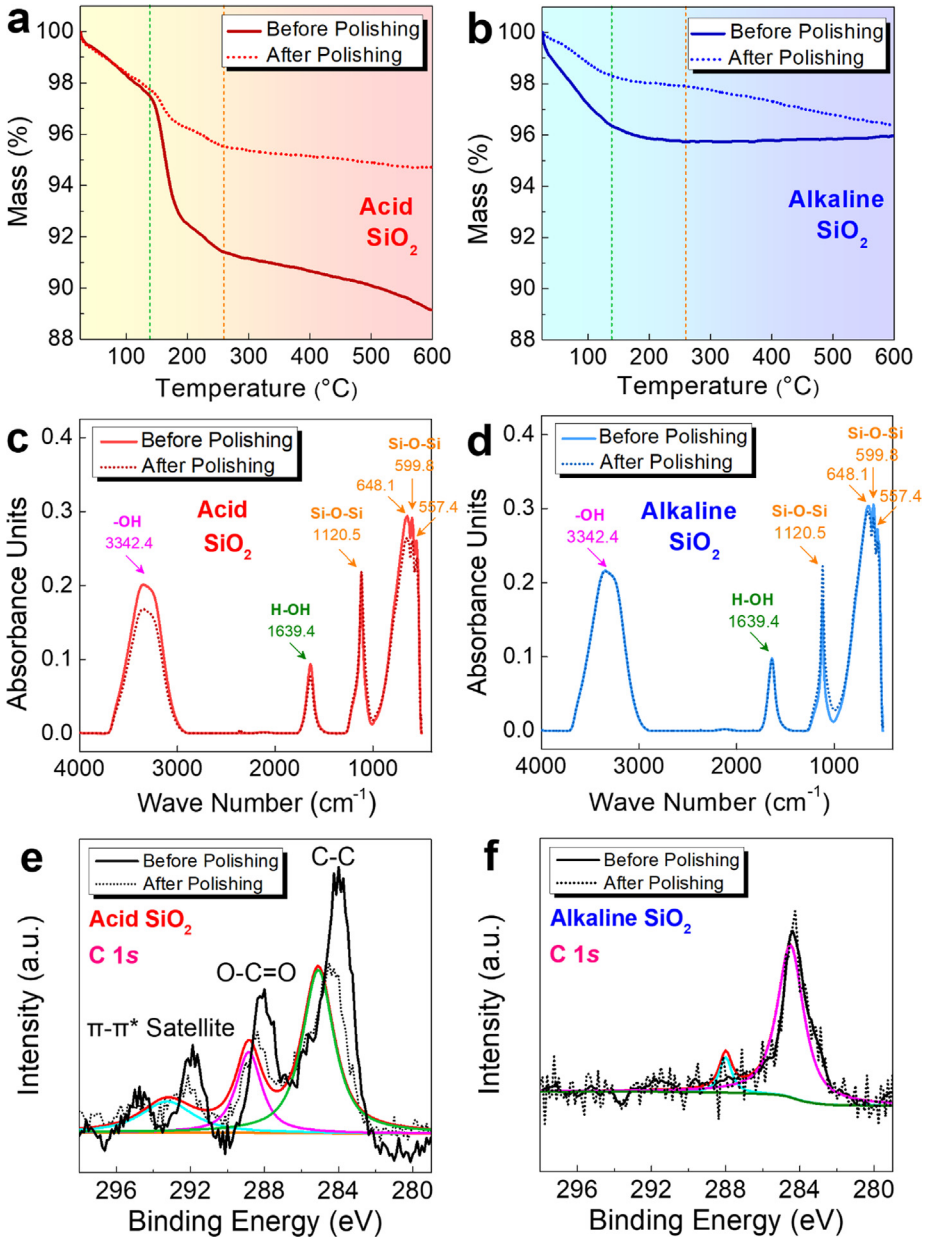

Fig. 3. Comparison of the analysis on acid and alkaline SiO_2 abrasives before and after 6 h polishing: TGA curves of (a) acid and (b) alkaline SiO_2 abrasives from RT to 600 °C; IR spectra of (c) acid and (d) alkaline SiO_2 abrasives, and XPS spectra of (e) acid and (f) alkaline SiO_2 abrasives for C 1*s*. The scales of Y-axes for (a) and (b) are unified for comparison and nuclear magnetic resonance spectra of (g) acid and (h) alkaline SiO_2 abrasives.

the consumption of active ingredients in the slurry. On the contrary, the MRR from the alkaline SiO_2 slurry remained almost stable or with a slight increase, indicating that there should be weak chemical reactions that occurred during CMP, and the mechanical polishing should dominate the material removal process when using alkaline SiO_2 slurry. This is reasonable because if there were obvious chemical reactions during CMP, with increasing the polishing time, the MRR should be reduced under circular conditions due to the continuous consumption of active ingredients in the slurry. After 6 h circular polishing, the MRR obtained by using the acid SiO_2 slurry remained above 5 μm h^{-1}, indicating that the durability of our acid SiO_2 slurry is relatively high. It should be noted that the decrease in MRR can be explained by both the consumption of active ingredients (which dominates the decrease of MRR), and effects of the rise in the *Z* and PDI values, as shown in Fig. 2(c) and (d), respectively. In a circular CMP process, the chemical products that were mechanically removed by the SiO_2 abrasives will stay and accumulate in the slurry, resulting in increases in detected *Z* and PDI. Fig. 2(e) and (f) show the variation of pH and *σ*, respectively. For the acid SiO_2 slurry, with increasing the polishing time, the pH keeps stable but the *σ* obviously decreases, indicating the consumption of active ingredients rather than H^+ ions. On the contrary, for alkaline SiO_2 slurry, the pH slightly decreases, indicating a consumption of the OH^- ion. Besides, compared with new slurries, the slurries standing for 1 month have same CMP performance, indicating our SiO_2 slurries possess high stabilities. The polished FS surfaces *via* different slurries are also provided in Fig. S4 for reference.

To explore the fundamental mechanisms behind such high MRR and surface quality in the FS substrate that have been prepared *via* our novel acid SiO_2 slurry process, we further studied the active ingredients in the slurry by comprehensive investigations including TGA, IR spectra, XPS, NMR spectra, and IC. Fig. 3(a) and (b) show the TGA curves of the acid and alkaline SiO_2 abrasives from room temperature (RT) to 600 °C, respectively. The abrasives were dried from their corresponding slurries in vacuum environment at RT. The abrasives before and after 6 h

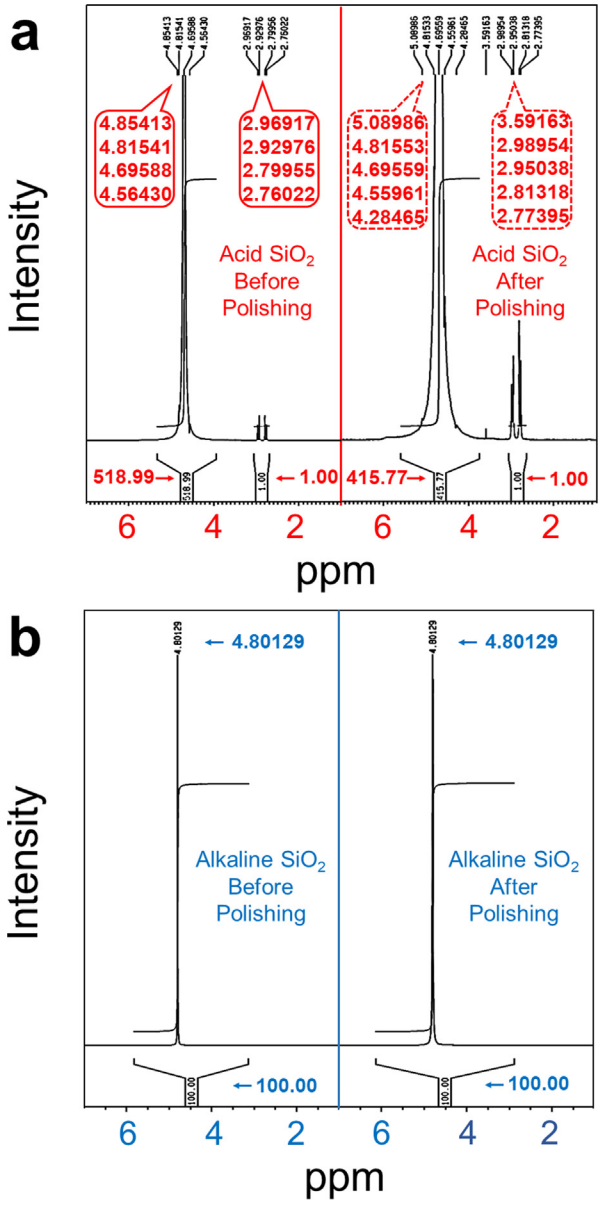

Fig. 4. Comparison of nuclear magnetic resonance spectra on (a) acid and (b) alkaline SiO_2 abrasives before and after 6 h polishing.

circular polishing were both included to study their differences. For acid SiO_2 abrasives, with increasing temperature, the mass gradually decreases, indicating that there was decomposition of the active ingredients, which mainly happened between 120 °C and 260 °C. Meanwhile, it is clear that with increasing temperature, compared with used acid SiO_2 abrasives (after polishing), the mass of new abrasives (before polishing) decreases at a higher rate after 120 °C, indicating more significant decompositions of the active ingredients. On the contrary, the mass of alkaline SiO_2 abrasives after 6 h polishing decreases at a much lower rate after 120 °C, indicating weak chemical reactions during CMP which results in low MRR. Fig. 3(c) and (d) show IR spectra of acid and alkaline SiO_2 abrasives before and after 6 h circular polishing, respectively. Compared with alkaline SiO_2 abrasives, it is clear that after 6 h polishing, the hydroxyl −OH peak becomes much weaker, indicating the consumption of −OH in acid SiO_2 slurry for 6 h polishing, confirming that the presence of the −OH plays a significant role in improving the MRR. These −OH groups originate mainly from the phenol (phenolic −OH) we added in the slurry as part of our new slurry design. Considering that phenol cannot exist in the alkaline slurry because the phenol can react with strong alkaline solution (even though we have added same amount of phenol in the alkaline slurry for comparison), the −OH groups in the alkaline slurry were entirely from the surface of the SiO_2 with limited concentration [25,29–33]. In this situation, there is not enough active −OH in the alkaline slurry during CMP, resulting in a much lower MRR than our novel acid slurry. In fact, −OH groups were also found as effective ingredients for polishing super-hard materials such as sapphire [23–28], SiC [25,29–33], and GaN [34–36] *via* SiO_2-based slurries, which can activate the bonds broken of Al−O [23–28], Si−C [25,29–33], Ga−N [34–36], and Si−O in glass [53], which is similar to our FS case. The IR results from the slurries standing for 1 month are the same as the new slurries as shown in Fig. S5, confirming the function of −OH and indicating that our slurries possess high stabilities.

To further study the active ingredients in the slurries, Fig. 3(e) and (f) show XPS spectra (focusing on C 1*s*) of the acid and alkaline SiO_2 abrasives before and after 6 h circular polishing, respectively. To exclude the error of XPS C 1*s* spectra caused by the organic pollution from the air, we performed the polishing experiment in a 1000 Super Clean Room to effectively prevent the absorption of suspended particulate materials from the surrounding air. After polishing, the FS wafers were placed in the vacuum bags for storage. Different from the results of the alkaline SiO_2 abrasives, there are typical C−C, O−C=O, and π-π* satellite peaks in our acid SiO_2 abrasives. The C−C and O−C=O peaks indicate the existence of aromatic and/or unsaturated structures, which mainly come from the phenol we added in the slurry as key components. It is clear that after 6 h polishing, the intensities of all these three peaks were significantly weakened, indicating an obvious consumption of phenol as key components to provide −OH in our acid SiO_2 slurry, and the phenol also plays a significant role in improving the MRR. The XPS results for Si 2*p* and O 1*s* *via* different slurries are also provided in Fig. S6 for reference.

To further confirm the function of aromatic and/or unsaturated structures on CMP of FS, Fig. 4(a) and (b) show the NMR spectra of acid and alkaline SiO_2 abrasives before and after 6 h circular polishing, respectively. Similarly, different from the results of alkaline SiO_2 abrasives, there are extra 1H NMR shifting detected from the acid SiO_2 abrasives which are related to the hydroxyl, aromatic and/or unsaturated structures (two ranges of 2.7–3.0 and 4.5–4.9, respectively), further confirming the existence of phenol in the slurry, which is responsible for improving the MRR of FS. After 6 h polishing *via* acid SiO_2 abrasives, more 1H NMR shifting can be detected in the range of 4.2–5.1 and 2.7–3.6, indicating the formation of chemical products. Besides, the much clearer NMR results from slurries standing for 1 month are similar to the new slurries as shown in Fig. S7, indicating that our slurries possess high stabilities for phenyl storing. For the removal mechanism of alkaline SiO_2 slurry, more evidence and discussion has been included in Fig. S8 of the Supporting Information.

To further explore the fundamental CMP mechanism *via* our novel SiO_2 slurries, we also performed detailed characterization on the FS substrate before and after 6 h polishing as shown in Fig. 5. Fig. 5(a) compares the TGA results of the FS substrate before and after 6 h polishing *via* both acid and alkaline SiO_2 slurries. It is clear that with increasing temperature, the mass of FS polished *via* alkaline SiO_2 slurry kept stable, similar to the results of pristine FS. On the contrary, the mass of FS polished *via* acid SiO_2 slurry gradually decreased, indicating the products resulting from the decomposition of phenol remained on the FS surface after CMP, fitting well with the TGA results for the acid SiO_2 abrasives shown in Fig. 3(a). Fig. 5(b) shows the IR spectra of FS substrate before and after 6 h polishing *via* both acid and alkaline SiO_2 slurries, measured at room temperature. It is clear that the IR spectrum of FS polished *via* alkaline SiO_2 slurry is very similar to that of pristine FS, indicating that there were weak chemical reactions occurred during CMP and there was limited chemical residual on the polished FS surface. On the contrary, the IR spectrum of FS polished *via* acid SiO_2 slurry possesses strong Si−O, Si−OH, and Si−O−Si peaks, indicating

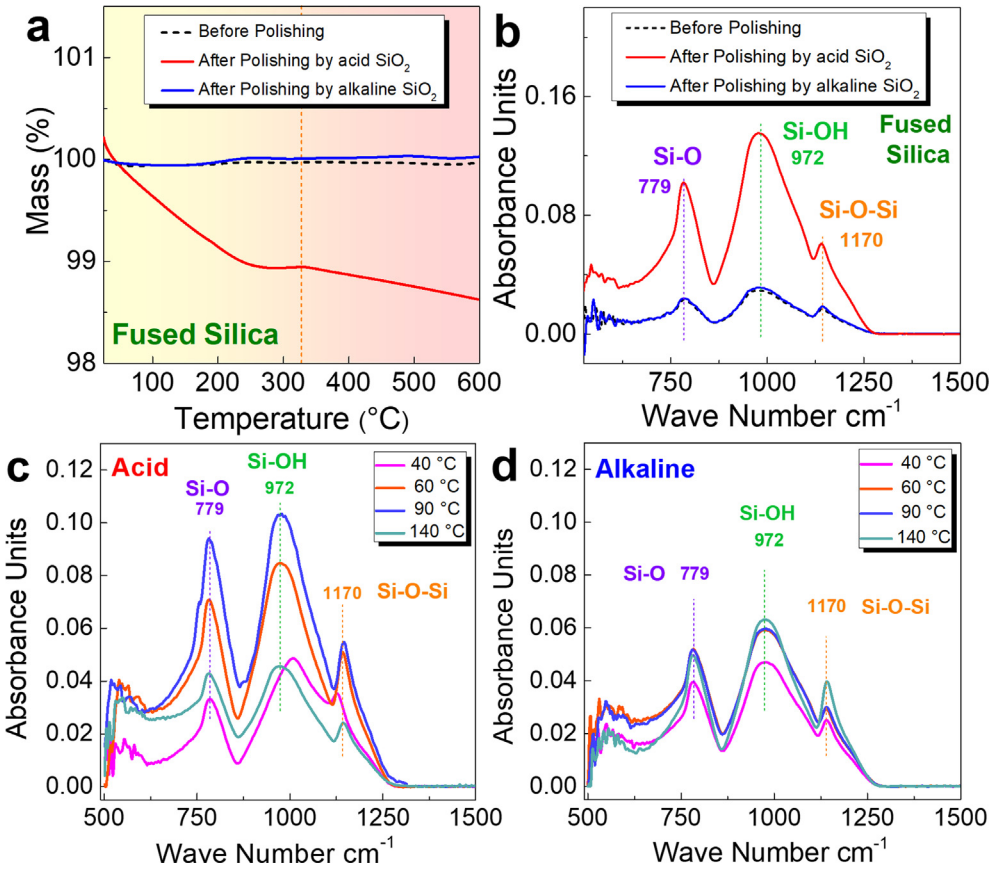

Fig. 5. Comparison of analysis on FS: (a) TGA curves and (b) IR spectra of FS before and after 6 h polishing by acid and alkaline SiO_2 slurries, the IR spectra was achieved at room temperature; IR spectra of FS soaked in (c) acid SiO_2 slurry and (d) alkaline SiO_2 slurry for 6 h at different temperatures. The scales of Y-axes for (c) and (d) have been combined for comparison.

that effective chemical reactions happened during CMP and there were considerable chemical residuals remaining on the polished FS surface. To confirm this, we further soaked the pristine FS substrates in both acid and alkaline SiO_2 slurries for 6 h at different temperatures, and their IR results are shown in Fig. 5(c) and (d), respectively. Compared with the results of FS soaked in the alkaline SiO_2 slurry, it is clear that after 1 h soaking in the acid SiO_2 slurry, the Si—O, Si—OH, and Si—O—Si peaks became more significant, indicating that effective chemical reactions occurred during soaking. Considering the peaks of Si—OH and Si—O became more significant than Si—O—Si peaks, the potential reaction can be described as:

$$\equiv Si{-}O{-}Si\equiv + -OH \rightarrow \equiv Si{-}O- + \equiv Si{-}OH \quad (2)$$

At the same time, it can be seen that by increasing the temperature up to 90 °C, the Si—O, Si—OH, and Si—O—Si peaks became more significant, indicating thermal activation that accelerated the chemical reactions. However, for the soaking temperature of 140 °C, the intensities of these peaks are similar to pristine FS, indicating that the decomposition of active ingredients happened at this temperature which resulted in limited chemical reactions, fitting well with the TGA results shown in Fig. 3(a). For the results of FS soaked in the alkaline SiO_2 slurry, it is clear that the heating can also contribute to accelerating the chemical reactions, but the effect was limited. At the same time, the intensities of peaks continued to increase slightly when the soaking temperature increased to 140 °C, double confirming that the key factor determining the high MRR is the presence of the phenolic −OH in our acid SiO_2 slurry during CMP. Furthermore, it should be noted that for CMP on FS, the electrostatic force between the abrasive particles and the FS may also play a significant role in the material removal besides the interfacial chemical reactions [54], and further studies are needed to explore the nature of such a unique acid SiO_2 slurry.

4. Conclusion

In summary, we simultaneously realized ultralow Ra of ~0.193 nm and high MRR of ~10.9 μm h^{-1} on the surface of FS using a novel acid SiO_2 slurry and advanced CMP techniques. This new approach delivered a ~900% improvement compared with the alkaline counterpart. Comprehensive characterizations demonstrated that the well-distributed SiO_2 abrasives with an average size of only ~80 nm lead to such high surface quality, and the phenolic hydroxyl in our acid SiO_2 slurry played a critical role in achieving such high MRR. Besides, our unique acid SiO_2 slurry is environmentally friendly with significantly high durability and stability, which is especially suitable for scale up to long-term industrial production. This work fills the gap in understanding the fundamental removal mechanisms associated with fused silica, and provides a new perspective for achieving high surface quality and removal efficiency in various materials.

Acknowledgement

This work was financially supported by the Science Challenge Project (No. TZ2016006-0503-03), China; National Natural Science Foundation of China (No. 51675348), China; Science and Technology Planning Project of Guangdong Province of China (2017B010112001), China; and the Science, Technology and Innovation Commission of Shenzhen Municipality (No. JCYJ20170817153703060), China. XLS thanks the IPRS for providing his PhD program, Australia.

Appendix A. Supplementary material

Supplementary data to this article can be found online at https://doi.org/10.1016/j.apsusc.2019.144041.

References

[1] F. Kotz, K. Arnold, W. Bauer, D. Schild, N. Keller, K. Sachsenheimer, T.M. Nargang, C. Richter, D. Helmer, B.E. Rapp, Nature 544 (2017) 337.
[2] W.S. Rodney, R.J. Spindler, JOSA 44 (1954) 677–679.
[3] C.D. Marshall, J.A. Speth, S.A. Payne, J. Non-cryst, Solids 212 (1997) 59–73.
[4] J. Xu, G. Pickrell, X. Wang, W. Peng, K. Cooper, A. Wang, IEEE. Photonic. Tech. L 17 (2005) 870–872.
[5] R. Roy, D.K. Agrawal, H.A. McKinstry, Annu. Rev. Mater. Sci. 19 (1989) 59–81.
[6] S. Susman, K. Volin, R. Liebermann, G. Gwanmesia, Y. Wang, Phys. Chem. Glasses 31 (1990) 144–150.
[7] A. Schreiber, B. Kühn, E. Arnold, F. Schilling, H. Witzke, J. Phys. D Appl. Phys. 38 (2005) 3242.
[8] S. Mishra, R. Mitra, M. Vijayakumar, J. Alloy. Compd. 504 (2010) 76–82.
[9] G. Bruin, G. Stegeman, A. Van Asten, X. Xu, J. Kraak, H. Poppe, J. Chromatogr. A 559 (1991) 163–181.
[10] A.K. Rai, H. Zhang, F.Y. Yueh, J.P. Singh, A. Weisberg, Spectrochim. Acta B 56 (2001) 2371–2383.
[11] N. Shibata, S. Shibata, T. Edahiro, Electron. Lett. 17 (1981) 310–311.
[12] S.B. Ali, B. Ghatak, S.D. Gupta, N. Debabhuti, P. Chakraborty, P. Sharma, A. Ghosh, B. Tudu, S. Mitra, M.P. Sarkar, Sensor. Actuat. B-Chem. 230 (2016) 791–800.
[13] F. He, Y. Cheng, Z. Xu, Y. Liao, J. Xu, H. Sun, C. Wang, Z. Zhou, K. Sugioka, K. Midorikawa, Opt. Lett. 35 (2010) 282–284.
[14] T. Suratwala, L. Wong, P. Miller, M. Feit, J. Menapace, R. Steele, P. Davis, D. Walmer, J. Non-cryst, Solids 352 (2006) 5601–5617.
[15] J. Neauport, L. Lamaignere, H. Bercegol, F. Pilon, J.-C. Birolleau, Opt. Express 13 (2005) 10163–10171.
[16] T. Suratwala, R. Steele, M. Feit, L. Wong, P. Miller, J. Menapace, P. Davis, J. Non-cryst, Solids 354 (2008) 2023–2037.
[17] P.A. Temple, W.H. Lowdermilk, D. Milam, Appl. Opt. 21 (1982) 3249–3255.
[18] T.I. Suratwala, P.E. Miller, J.D. Bude, W.A. Steele, N. Shen, M.V. Monticelli, M.D. Feit, T.A. Laurence, M.A. Norton, C.W. Carr, J. Am. Ceram. Soc. 94 (2011) 416–428.
[19] S.R. Runnels, L.M. Eyman, J. Electrochem. Soc. 141 (1994) 1698–1701.
[20] M. Forsberg, Microelectron. Eng. 77 (2005) 319–326.
[21] J. Steigerwald, S. Murarka, R. Gutmann, D. Duquette, Mater. Chem. Phys. 41 (1995) 217–228.
[22] L. Wang, K. Zhang, Z. Song, S. Feng, Appl. Surf. Sci. 253 (2007) 4951–4954.
[23] Y. Zhou, G. Pan, X. Shi, H. Gong, L. Xu, C. Zou, J. Mater. Sc. Mater. El. 26 (2015) 9921–9928.
[24] Y. Zhou, G. Pan, H. Gong, X. Shi, C. Zou, Colloid. Surface A 513 (2017) 153–159.
[25] Y. Zhou, G. Pan, X. Shi, S. Zhang, H. Gong, G. Luo, Tribol. Int. 87 (2015) 145–150.
[26] L. Xu, C. Zou, X. Shi, G. Pan, G. Luo, Y. Zhou, Appl. Surf. Sci. 343 (2015) 115–120.
[27] X. Shi, L. Xu, Y. Zhou, C. Zou, R. Wang, G. Pan, Nanoscale 10 (2018) 19692–19700.
[28] X. Shi, G. Pan, Y. Zhou, L. Xu, C. Zou, H. Gong, Surf. Coat. Tech. 270 (2015) 206–220.
[29] X. Shi, G. Pan, Y. Zhou, Z. Gu, H. Gong, C. Zou, Appl. Surf. Sci. 307 (2014) 414–427.
[30] X. Shi, G. Pan, Y. Zhou, C. Zou, H. Gong, Appl. Surf. Sci. 284 (2013) 195–206.
[31] Y. Zhou, G. Pan, X. Shi, L. Xu, C. Zou, H. Gong, G. Luo, Appl. Surf. Sci. 316 (2014) 643–648.
[32] Y. Zhou, G. Pan, X. Shi, H. Gong, G. Luo, Z. Gu, Surf. Coat. Tech. 251 (2014) 48–55.
[33] G. Pan, Y. Zhou, G. Luo, X. Shi, C. Zou, H. Gong, J. Mater. Sci. Mater. El. 24 (2013) 5040–5047.
[34] X. Shi, C. Zou, G. Pan, H. Gong, L. Xu, Y. Zhou, Tribol. Int. 110 (2017) 441–450.
[35] C. Zou, G. Pan, X. Shi, H. Gong, Y. Zhou, P.I. Mech, Eng. J-J. Eng. 228 (2014) 1144–1150.
[36] H. Gong, G. Pan, Y. Zhou, X. Shi, C. Zou, S. Zhang, Appl. Surf. Sci. 338 (2015) 85–91.
[37] R. Sabia, H.J. Stevens, Mach. Sci. Technol. 4 (2000) 235–251.
[38] Q. Luo, J. Lu, X. Xu, F. Jiang, Ceram. Int. 43 (2017) 16178–16184.
[39] N.J. Rogers, N.M. Franklin, S.C. Apte, G.E. Batley, B.M. Angel, J.R. Lead, M. Baalousha, Environ. Chem. 7 (2010) 50–60.
[40] M.L. López-Moreno, G. de la Rosa, J.A. Hernández-Viezcas, J.R. Peralta-Videa, J.L. Gardea-Torresdey, J. Agr. Food Chem. 58 (2010) 3689–3693.
[41] S. Recillas, A. Garcia, E. Gonzalez, E. Casals, V. Puntes, A. Sanchez, X. Font, Desalination 277 (2011) 213–220.
[42] I.-S. Kim, M. Baek, S.-J. Choi, J. Nanosci. Nanotechno. 10 (2010) 3453–3458.
[43] Z. Zhang, J. Cui, J. Zhang, D. Liu, Z. Yu, D. Guo, Appl. Surf. Sci. 467 (2019) 5–11.
[44] Z. Zhang, Z. Shi, Y. Du, Z. Yu, L. Guo, D. Guo, Appl. Surf. Sci. 427 (2018) 409–415.
[45] Z. Zhang, S. Huang, L. Chen, B. Wang, B. Wen, B. Zhang, D. Guo, Appl. Surf. Sci. 416 (2017) 891–900.
[46] Z. Zhang, B. Wang, S. Huang, B. Wen, S. Yang, B. Zhang, C.-T. Lin, N. Jiang, Z. Jin, D. Guo, Mater. Des. 106 (2016) 313–320.
[47] Z. Zhang, B. Wang, P. Zhou, D. Guo, R. Kang, B. Zhang, Sci. Rep. 6 (2016) 22466.
[48] Z. Zhang, B. Wang, P. Zhou, R. Kang, B. Zhang, D. Guo, Sci. Rep. 6 (2016) 26891.
[49] Z.L. Wang, X. Feng, J. Phys. Chem. B 107 (2003) 13563–13566.
[50] C. Kang, D. Guo, X. Zhang, C. Zou, G. Pan, ECS J. Solid State Sci. 8 (2019) 7–11.
[51] X. Shi, L. Guo, Y. Bai, L. Qiao, Appl. Surf. Sci. 257 (2011) 7238–7244.
[52] L. Gou, X. Shi, X. Zhao, Y. Bai, L. Qiao, Surf. Coat. Tech. 206 (2012) 4099–4105.
[53] L.M. Cook, J. Non-cryst, Solids 120 (1990) 152–171.
[54] W. Yan, Z. Zhang, X. Guo, W. Liu, Z. Song, ECS J. Solid State Sci. 4 (2015) 108–111.